GENERALIFE: Synergistic Raman Lidar and Fluorescence Spectroscopy for Enhanced Aerosol Typing

S. Fernández-Carvelo[a,b], A. Yadav[c], B. Tatarov[c], P. Ortiz-Amezcua[d], A. del Águila[a,b], J.A. Bravo-Aranda[a,b], E. Bazo[a,b], A. Valenzuela[a,b], D. Müller[c] and L. Alados-Arboledas[a,b]

[a]*Andalusian Institute for Earth System Research (IISTA), University of Granada, Granada, Spain*
[b]*Department of Applied Physics, University of Granada, Granada, Spain*
[c]*Department of Physics, Astronomy and Mathematics, University of Hertfordshire, College Lane, Hatfield, UK*
[d] *Department of Physics, University Carlos III of Madrid, Madrid, Spain*
Lead Author e-mail address: solfcarvelo@ugr.es

Abstract: Atmospheric aerosol particles play a key role in climate and air quality, yet their characterization remains challenging due to strong variability and complex composition. We present an advanced aerosol characterization approach that combines multi-wavelength Raman lidar optical retrievals with broadband and spectrally resolved fluorescence observations performed at the SPECTRALAB facility of the AGORA observatory (Granada, Spain). Measurements were conducted using GENERALIFE, a combined spectroscopic lidar system integrating the multi-wavelength Raman lidar ALHAMBRA with a dedicated fluorescence module operated in dual near- and far-field configurations. A comprehensive and traceable calibration and preprocessing strategy ensures the quantitative reliability of the spectroscopic measurements. The capabilities of the system are demonstrated through a major biomass-burning outbreak affecting southern Europe and a subsequent Saharan dust intrusion observed during the same week in August 2025, highlighting the added value of fluorescence variability for aerosol discrimination.

1. Introduction

Atmospheric aerosol particles play a key role in the Earth's radiative balance and air quality, but their characterization remains challenging due to strong variability driven by emission sources, atmospheric processing, and mixing state. Lidar techniques provide vertically resolved observations and have become essential tools for aerosol profiling and monitoring [1,2]. Raman and advanced lidar systems enable the retrieval of key optical properties, such as backscatter, extinction, lidar ratios, Ångström exponents, and depolarization, significantly improving aerosol typing and source attribution [3]. Further developments, including HSRL, multi-species Raman, and fluorescence lidar, have expanded capabilities toward aerosol and cloud characterization [4–6]. However, optical properties alone are often insufficient to constrain aerosol chemical composition, particularly in layered, aged, or mixed conditions. Laser-induced fluorescence provides complementary, chemically sensitive information linked to aerosol constituents. Spectrally resolved fluorescence reveals distinct variability regimes: biomass-burning aerosols typically exhibit strong, height-dependent spectral variability with height and time, whereas mineral dust exhibits weak and spectrally stable induced fluorescence. This contrast enhances aerosol discrimination and supports the detection of optically thin layers and aerosol–cloud interaction studies [7–11]. Building on this approach, the present work extends a multi-wavelength Raman lidar framework by incorporating broadband near-field and spectrally resolved far-field fluorescence observations. The methodology is demonstrated for a major wildfire outbreak over the western Iberian Peninsula followed by a Saharan dust intrusion during the same week, providing an ideal test case for the discrimination of contrasting aerosol types.

2. Instrumentation

The experimental results presented in this study were obtained using GENERALIFE, a combined spectroscopic lidar system integrating the Dual-LMRD multi-wavelength Raman lidar ALHAMBRA (Raymetrics S.A.,

Greece) with a dedicated spectroscopic module. GENERALIFE is operated by the University of Granada at the SPECTRALAB facility of the Andalusian Global ObseRvatory of the Atmosphere (AGORA), southern Spain. Measurements were performed at the University of Granada (UGR) station in Granada (37.16° N, 3.61° W, 680 m a.g.l.), a site suitable for observing a wide range of aerosol scenarios, including urban pollution, biomass burning (BBA), mineral dust, and mixed aerosol layers. ALHAMBRA is part of both ACTRIS [1] and EARLINET [2]. The system comprises two complementary subsystems: a near-field biaxial configuration optimized for boundary-layer observations with elastic and N_2 vibrational Raman channels, and a far-field coaxial configuration extending measurements to the upper troposphere and lower stratosphere, including elastic and O_2–N_2 pure rotational Raman channels. Both subsystems are equipped with depolarization capabilities at 355 and 532 nm. Fluorescence measurements within GENERALIFE are implemented using two complementary approaches. Broadband fluorescence is detected in the near-field subsystem using an interference filter (Semrock BrightLine® 470/100 nm), while spectrally resolved fluorescence in the far-field subsystem is measured with a Newport Oriel M125-77400 spectrometer optically coupled to ALHAMBRA via an optical fiber [5]. The dispersed spectra are recorded using a Licel SP32 multispectral detector equipped with a 32-channel multi-anode photomultiplier (Hamamatsu H7260-103). During spectroscopic operation, the far-field subsystem emits laser pulses exclusively at 355 nm, with the 532 and 1064 nm emissions suppressed. The spectrometer was configured with a 1200 grooves mm^{-1} grating and a 1000 µm entrance slit, providing a spectral resolution of ~6.2 nm over the 351.5–543.5 nm range. Elastic scattering was partially suppressed using a narrow bandpass filter centered at 355 nm (2 nm FWHM, OD6 blocking). In situ aerosol optical properties were measured at AGORA using an integrating nephelometer (TSI 3563) at 450, 550, and 700 nm and a multiwavelength aethalometer (AE33, Magee Scientific) operating between 370 and 950 nm, both with 1 min temporal resolution. All in situ measurements were previously calibrated and corrected [12].

3. Methodology

For lidar measurements, standard preprocessing was applied [1,2]. For the spectroscopic data, a comprehensive and traceable calibration strategy was implemented to ensure quantitative reliability. Background subtraction and zero-bin correction were applied to the raw signals. Inter-channel crosstalk was quantified and corrected, and photon-counting dead-time effects were corrected for signal intensities exceeding 10 MHz. The wavelength-dependent efficiency of the detector–grating system was characterized through dedicated measurements, yielding a normalized efficiency curve that slightly differs from the theoretical response provided by the manufacturers. Spectral wavelength calibration was performed using mercury lamp measurements by identifying reference emission lines and applying polynomial fitting to derive calibrated wavelengths and channel-dependent spectral resolution. The different atmospheric scenaries were characterized based on intensive and extensive lidar optical properties and simultaneous broadband and spectral fluorescence data. Fluorescence analysis focuses on selected aerosol layers, examining spectral trends and characteristic emission peaks as a function of height and aerosol type. Data from HYSPLIT backward trajectories [11], AERONET observations [12] and FIRMS fire detections [13] together with co-located in situ measurements were also used.

4. Results

Figure 1 shows the temporal evolution of in situ aerosol optical properties during August 2025, including multiwavelength scattering coefficients (450, 550, and 700 nm) and absorption at 370 nm. Two major aerosol events are identified within the same week: a biomass-burning aerosol (BBA) episode (20–22 August 2025) and a Saharan dust intrusion (25–28 August 2025). The BBA event exhibits strong wavelength-dependent scattering, indicative of a dominant fine-mode aerosol population, whereas the dust intrusion shows similarly high scattering levels but much weaker spectral dependence, consistent with coarse mineral particles. Absorption peaks during both

episodes, confirming their radiative relevance.

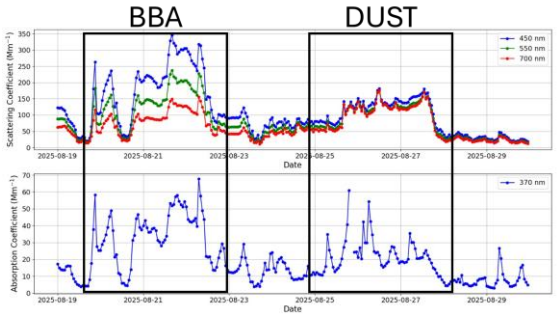

Figure 1. Time series of aerosol scattering and absorption coefficient, measured in August 2025.

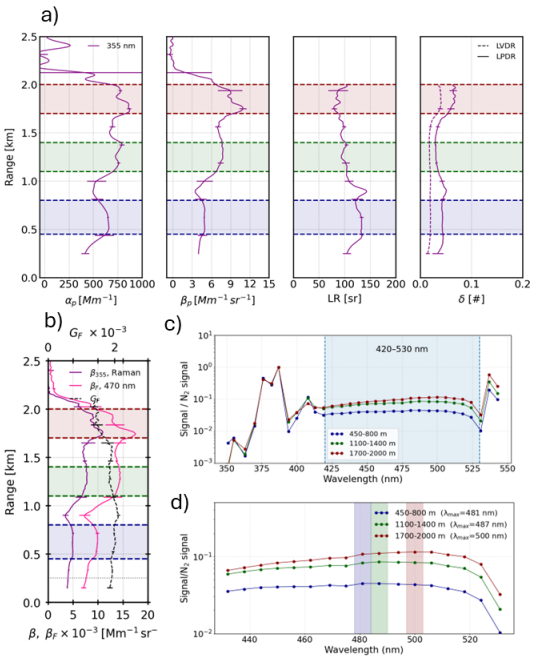

Figure 2. Optical and fluorescence lidar observations during the biomass-burning aerosol event (20–22 August 2025).

Figure 2 summarizes the vertically resolved lidar and fluorescence observations during the BBA event. Multiple aerosol layers are detected between approximately 0.4 and 2.0 km above ground level. Extinction and backscatter profiles indicate a vertically stratified smoke structure, with high moderate ratios and low particle depolarization ratios (<10%), consistent with a dominant fine-mode, weakly depolarizing biomass-burning aerosol population (Figure 2a). Enhanced fluorescence backscatter and fluorescence capacity closely coincide with the main aerosol layers, confirming a substantial contribution from fluorescent organic compounds. The observed broadband fluorescence backscatter reaches values on the order of ~10^{-3} Mm^{-1} sr^{-1} (Figure 2c), which lies within the wide range reported for biomass-burning aerosol in recent broadband fluorescence lidar studies, where fluorescence signals vary strongly depending on aerosol load and plume characteristics [4-7]. The present episode originates from northwestern Spain and Portugal and is associated with a shorter transport time, suggesting a more regionally influenced and relatively fresh smoke mixture. Spectrally resolved fluorescence measurements reveal a broad emission spectrum with a maximum around 500 nm, characteristic of BBA excited at 355 nm (Figures 2c and 2d). Nevertheless, spectrometric lidar observations demonstrate that BBA fluorescence spectra can exhibit pronounced variability, including height-dependent spectral shifts, reflecting differences in source regions, aging, and mixing state. This complexity is consistent with the documented spread in retrieved lidar ratios for biomass-burning aerosol, emphasizing that smoke layers are often chemically and optically heterogeneous rather than uniform aerosol types [7].

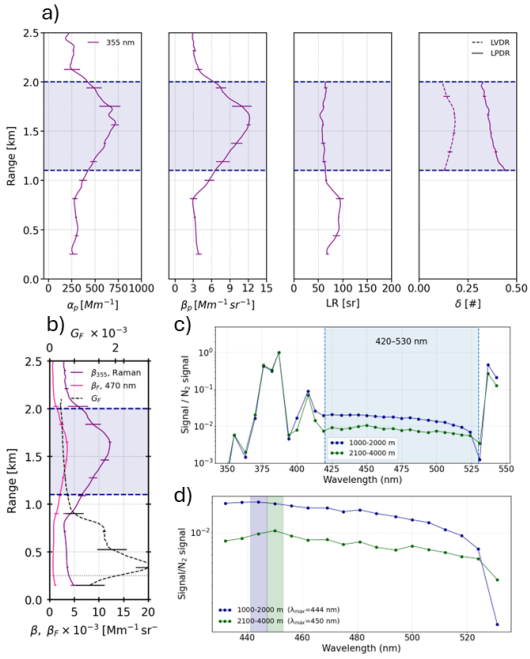

Figure 3. Same as Figure 2, but for the Saharan mineral dust event (25–28 August 2025).

Figure 3 presents the Saharan mineral dust event analyzed with the same framework. A single, well-defined aerosol layer is observed between approximately 1.1 and 2.0 km above ground level, showing smoother and more homogeneous vertical structures than in the

BBA case. Retrieved lidar ratios are moderate even though within the documented variability for Saharan dust, while particle depolarization ratios strongly exceed 30% (up to ~50%), clearly reflecting the dominance of coarse, non-spherical mineral dust particles (Figure 3a). In contrast to the smoke episode, fluorescence backscatter and fluorescence capacity remain weak throughout the dust layer, with fluorescence backscatter coefficients lower than those for BBA but still on the order of ~10^{-4} Mm^{-1} sr^{-1} (Figure 3b). Spectrally resolved fluorescence measurements exhibit a distinctly different signature compared to BBA, with maxima shifted toward the blue–cyan range around ~440–450 nm and a pronounced decrease toward longer wavelengths (Figures 3c and 3d). This spectral behaviour also closely agrees with the dust spectra reported in recent studies in which is shown that Saharan dust fluorescence is generally skewed toward short wavelengths and remains weak in terms of spectral fluorescence capacity. Only minor height-dependent variations are observed, suggesting that dust fluorescence can be mainly controlled by mineralogical composition. Nevertheless, some degree of mixing during transport cannot be excluded. Overall, the results are consistent with the substantial variability documented for Saharan dust optical properties, including a widespread in retrieved lidar ratios depending on source regions and atmospheric processing [7].

5. Conclusions

This study demonstrates the potential of combining multi-wavelength Raman lidar with spectrally resolved fluorescence measurements to improve aerosol characterization within the GENERALIFE framework. BBA events exhibit strong and spectrally variable fluorescence, whereas mineral dust shows weak and comparatively stable fluorescence signatures. These preliminary results indicate that fluorescence spectroscopy provides complementary, sensitive composition information beyond conventional lidar optical properties. Future work will expand the dataset and include chemical composition measurements to further constrain fluorescence-based aerosol typing and their relevance for network-oriented observations within ACTRIS and EARLINET.

6. References

[1] P. Laj et al., “ACTRIS: The European research infrastructure supporting atmospheric science,” Bull. Amer. Meteor. Soc. 105, E1098 (2024).
[2] G. Pappalardo et al., “EARLINET: towards an advanced sustainable European aerosol lidar network,” Atmos. Meas. Tech. 7, 2389 (2014).
[3] A. del Águila et al., “Aerosol type classification with machine learning applied to multiwavelength lidar data from EARLINET,” Atmos. Chem. Phys. 25, 12549 (2025).
[4] I. Veselovskii et al., “Impact of water uptake on fluorescence of atmospheric aerosols,” Atmos. Meas. Tech. 18, 6039 (2025).
[5] B. Gast et al., “Invisible aerosol layers: improved lidar detection by laser-induced aerosol fluorescence,” Atmos. Chem. Phys. 25, 3995 (2025).
[6] M. Gidarakou et al., “Profiling pollen and biomass burning particles using laser-induced fluorescence lidar during the PERICLES campaign,” Atmos. Chem. Phys. 26, 923 (2026).
[7] J. Reichardt et al., “Fluorescence spectra of atmospheric aerosols,” Atmos. Chem. Phys. 25, 5857 (2025).
[8] B. Tatarov and D. Müller, “LITES: rotational Raman spectra measured by high-resolution spectroscopy lidar,” Opt. Lett. 46 (2021).
[9] A. Yadav et al., “Characterizing Saharan dust transported to the UK through lidar ratio, depolarization, and spectroscopic measurements,” Atmos. Environ. 363, 121613 (2025).
[10] E. Bazo et al., “Phase matrix characterization of long-range-transported Saharan dust,” Atmos. Chem. Phys. 25, 6325 (2025).
[11] NOAA ARL, “HYSPLIT,” https://www.arl.noaa.gov/hysplit/.
[12] NASA, “AERONET,” https://aeronet.gsfc.nasa.gov/.
[13] NASA, “FIRMS,” https://firms.modaps.eosdis.nasa.gov/.

Acknowledgements

This work is part of the Spanish national projects PID2020-120015RB-100, PID2022-142708NA-I00, PID2023-151668OB-I00, and PID2023-151817OA-I00, funded by MICIU/AEI/10.13039/501100011033; the strategic network RED2024-153891-E; the IRISCC EUproject (Grrant agreement ID: 101131261); and by UGR through the Scientific Unit of Excellence: Earth System (UCE-PP2017-02) and the Visiting Scholar PPVS2024-06. A. del Águila is part of the Juan de la Cierva programme through grant JDC2022-048231-I, funded by MCIN/AEI/10.13039/501100011033 and by the European Union (NextGenerationEU/PRTR). Sol Fernández-Carvelo received funding from the Spanish Ministry of Research and Innovation (Agencia Estatal de Investigación) through grant PRE2021-098351, co-funded by the European Social Fund Plus. This work has been developed within the framework of ACTRIS. Part of this work was supported by the COST Action EARLICOST (CA24135), supported by COST (European Cooperation in Science and Technology).